

Effect of Initial Conditions on Aerodynamic and Acoustic Characteristics of High Subsonic Jets from Sharp Edged Circular Orifice

Murugan, K. N. and Sharma, S. D.

NOMENCLATURE

Symbol	Quantity	Units
c	Speed of sound	m/s
D	Exit diameter	mm
f	Frequency	Hz
k	Acoustic wave number ($2\pi f/c$)	
m	Mass flow rate	kg/s
M	Mach Number	
P_{rms}	Root mean square pressure	Pa
p	Pressure fluctuations	Pa
r	Radial distance from jet geometric axis	mm
SPL	Sound Pressure Level = $20 \log \left(\frac{P_{rms}}{P_{ref}} \right)$	dB rel 20 μ Pa
St_D	Strouhal Number = fD / U_j	
u	Axial mean velocity	m/s
U_j	Jet exit Velocity	m/s
y	Distance between microphone location and shear layer center	m
ρ	Density	kg/m ³

Abstract—The present work involves measurements to examine the effects of initial conditions on aerodynamic and acoustic characteristics of a Jet at $M=0.8$ by changing the orientation of sharp edged orifice plate. A thick plate with chamfered orifice presented divergent and convergent openings when it was flipped over. The centerline velocity was found to decay more rapidly for divergent orifice and that was consistent with the enhanced mass entrainment suggesting quicker spread of the jet compared with that from the convergent orifice. The mixing layer region elucidated this effect of initial conditions at an early stage – the growth was found to be comparatively more pronounced for the divergent orifice resulting in reduced potential core size. The acoustic measurements, carried out in the near field noise region outside the jet within potential core length, showed the jet from the divergent orifice to be less noisy. The frequency spectra of the noise signal exhibited that in the initial region of comparatively thin mixing layer for the convergent orifice, the peak registered a higher SPL and a higher frequency as well. The noise spectra and the mixing layer development suggested a direct correlation between the coherent structures developing in the initial region of the jet and the noise captured in the surrounding near field.

Keywords—Convergent orifice jet, Divergent orifice jet, Mass entrainment, mixing layer, near field noise, frequency spectrum, SPL, Strouhal number, wave number, reactive pressure field, propagating pressure field.

I. INTRODUCTION

A jet can be issued from either a smoothly contoured nozzle or a long pipe nozzle (straight as well as tapered) or an orifice. Each of these configurations is expected to create different initial condition due to varying viscous effects at the exit. The geometric shape of the exit, circular or non-circular, also plays a role in determining the initial conditions. Since onset of instabilities in jet flow and its further development is carried over from the initial flow conditions prevailing at the

Viswanathan and Clark [1] studied the effects of nozzle internal contours on jet acoustics. Three different types of nozzles (conic, ASME and cubic) with equal exit diameter were tested at the same flow speed. The boundary layer at the exit was vastly different – thin for the cubic nozzle and thick for the conic nozzle. However, there was no difference found in the noise produced from these two nozzles and the ASME nozzle was found to be more noisy. Arakeri et al.[2] found that the noise produced by a conic nozzle depended on the state of the boundary layer at the exit – laminar boundary layer produced more noise than the turbulent boundary layer. Similar observations were made by Zaman [3] for a nozzle with smooth contour and by Maesterllo and McDaid [4] for a circular pipe nozzle. The beveled exit of the nozzle was found to alter the development of coherent structures in the initial region of the jet and this condition resulted in better noise reduction compared to a circular nozzle as reported by Viswanathan [5]. Jets from sharp edged orifice are least expected to show any influence of the initial boundary layer. There have been studies on sharp edged orifice jets by Quinn and J. Militzer [6], Mi et al [8], Quinn [9] and Mi et al [10]; however, they have been focused largely on the hydrodynamic

K. N. Murugan is Research Scholar in Department of Aerospace Engineering, Indian Institute of Technology Bombay, Mumbai, India.(E-mail: knmurugan@ aero.iitb.ac.in).

Sharma, S. D., Professor in in Department of Aerospace Engineering, Indian Institute of Technology Bombay, Mumbai, India.(E-mail: sds@ aero.iitb.ac.in).

aspects and compared with the jets from other configurations. It is surprising that despite its distinctly different hydrodynamic characteristic, the jet from sharp edged orifice has not become candidate for the aero-acoustics studies.

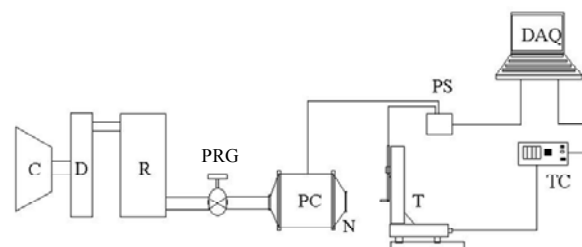
It is a matter of inference from the available data that a sharp edged orifice produces a jet with vena contracta which results in converging-diverging streamlines in the initial region. It is felt that formation of vena contracta may have stronger effects not only on the hydrodynamic/aerodynamic characteristics of jet but also on its acoustic characteristics. The objective of the present work is, therefore, to experimentally study the sharp edged orifice jet in order to find correlation between its aerodynamic and acoustic characteristics

II. EXPERIMENTAL METHOD

Figure 1 shows the schematic diagram of the test setup used for the present study. A high pressure reservoir with 30 m³ capacity is charged with dry air by means of a two-stage reciprocating compressor which is driven by a 90 hp electric motor. The compressor delivers 5.7 m³ of air per minute at a pressure of 14 kg/cm² which is adequate for a 50 mm diameter nozzle running continuously at choked condition. A globe valve is manually operated to regulate the constant mass flow rate in order to maintain the desired pressure in a cylindrical plenum chamber which is 332 mm in diameter and 550 mm long. The plenum chamber is connected to a conical end having an opening of 36 mm diameter with a 110 mm diameter flange to facilitate fixing of a nozzle or an orifice plate to produce a jet. A 5 mm thick steel plate was bored and chamfered to make a sharp edged orifice with a diameter, D, of 20 mm size. The same orifice plate was used either as a convergent orifice or as a divergent orifice simply by changing its orientation as shown in Fig.2.

A miniature Pitot probe was constructed out of stainless steel hypodermic tube with outer diameter of 0.7 mm. The mouth of the Pitot probe was chamfered using 0.6 mm drill-bit to minimize the flow spillage around the free tip and also to make the probe less sensitive to the flow angle. A larger diameter stem was provided in telescopic fashion so as to provide rigidity to stand the impact of the high speed jet. The Pitot probe was mounted on a Dantec Dynamics computerized automatic traverse. It can traverse a distance of 610 mm along each of three orthogonal directions with the minimum step size of 0.01 mm at a speed of 25 mm/s. With reference to the ambient atmospheric pressure, the plenum chamber pressure was calculated using isentropic flow relations for a predetermined Mach number of the flow at the orifice exit plane and was maintained by means of pressure regulating value. Pressures were registered by Pressure Systems make transducers, PSI model 9116 with 16 channels. The pressure transducer is capable of measuring 103 kPa gauge pressure with an accuracy of $\pm 0.05\%$ of full scale. It uses NUSS software for acquiring the data at a scanning rate of 500 samples per second. A 6.53 mm B& K 4939 free-field condenser microphone was used for the acoustic measurement. The microphone was powered by Nexus model

2690-0S2 signal conditional amplifier. The microphone has an open circuit sensitivity of 4.5 mV/pa and flat frequency response up to 100 kHz. The microphone was periodically calibrated using a B&K 4226 Multifunction acoustic calibrator. National Instrument DAQ PCI-6259 card and LabView software were used for acoustic data acquisition and post processing.



C- Compressor, D –Dryer, R-Reservoir, PRG- Pressure Regulating Valve, PC- Plenum Chamber, N- Nozzle attachment, T-Traverse with pitot-tube, TC- Traverse Controller, PS – Pressure Scanner, DAQ- Data Acquisition system.

Fig. 1 Schematic layout of experimental setup

Experiments were conducted at the plenum chamber temperature of about 300 ± 2 K and pressure of 1.524 times the ambient value to produce a free jet at $M=0.8$. The tests comprised of measurements of mean pitot pressures inside the jet and acoustic pressure fluctuations outside the jet. The pitot pressures were measured along the jet centerline and across the jet in radial direction at several streamwise locations. The traverse of the pitot probe in the radial direction was performed in a step of 2 mm to take care of high velocity gradient in the transverse plane. The acoustic pressure fluctuations were measured in close proximity of the jet covering the entire potential core length with the microphone pointing towards the jet centerline in 90° angular position. Figure 3 illustrates the matrix of microphone locations with a grid of $0.5D \times 0.5D$ in axial and radial directions. The lowest row was aligned nearly parallel to the mixing layer edge at an angle of about 7 degree to the jet axis having the coordinates of the first and the last stations being (1.5D, 1.22D) and (6D, 1.8D), respectively. These locations were determined on the basis of the pitot probe measurements. The Reynolds number for the jet flow was calculated to be 2.72×10^5 , based on the orifice diameter and the centerline velocity just downstream of the orifice plate. It may be noted that the volume of the settling chamber is just 0.16 % of that of the high pressure reservoir. Further, the settling chamber pressure required for the present experiments is only about 5 % of the fully charged reservoir pressure. Thus, the control of the pressure regulating valve could be managed manually with ease and precision enabling the settling chamber pressure maintained within about $\pm 0.29\%$. Taking into account the measurement uncertainty for such experimental conditions, the jet centerline velocity at the orifice exit plane was calculated to be 261.28 ± 0.11 m/s.

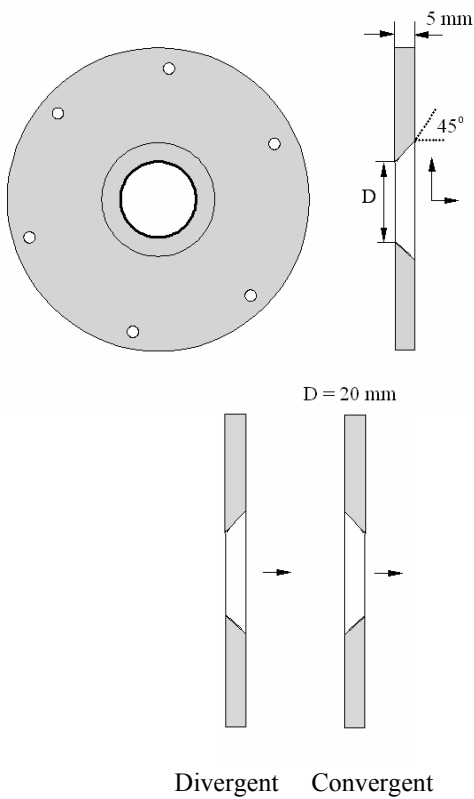


Fig. 2 Orifice plate and its arrangement for convergent and divergent configurations

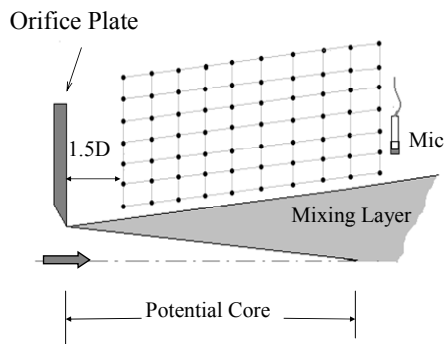


Fig. 3 Sketch showing locations for placement of microphone for near field acoustics measurements

III. RESULTS AND DISCUSSION

Figure 4 shows comparison of the centerline velocity distribution in the jets from the convergent and divergent orifices. Since the static pressure in the jet was assumed to be same as the atmospheric pressure, the velocity calculated within the potential core fails to capture the effect of vena contracta and remains constant. Jets produced from orifice are known to form vena contracta where the cross-sectional area and the static pressure are minimum and the velocity is

maximum. The plot suggests that the potential core length is about 4 diameters, however, the one for the divergent orifice being slightly shorter. Further downstream, the velocity variation shows typical decay trend. The rate of decay varies along the streamwise direction and seems to reach its maximum around x/D of 10. Of the two, the velocity for the convergent orifice jet is seen to be consistently higher. Suggesting that the divergent orifice promotes better mixing and as a consequence its jet spread should be greater. However, this was hard to discern from comparison of the velocity profiles. A better indicator would be the entrainment of mass into the jet that plays a vital role in its development. Figure 5 illustrates this point very clearly. Data showing a significantly higher mass flow entrained in to the divergent orifice jet corroborate the results previously shown in Fig. 4..

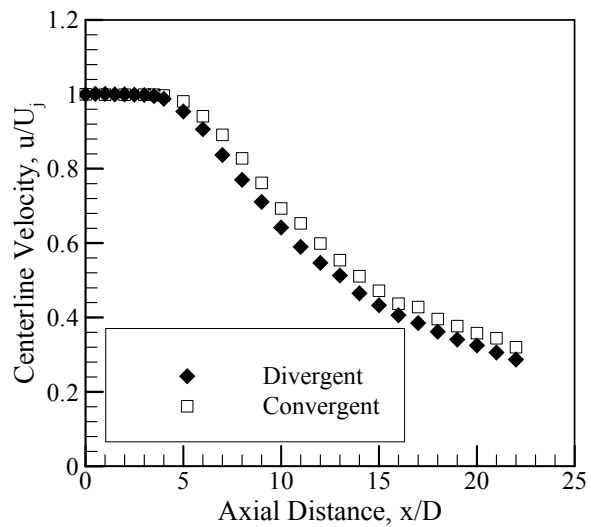


Fig. 4 Velocity distributions along jet centerline

The entrainment mass flow rate was calculated from the distribution of velocity, measured along the vertical axis and averaged over equal radial distances, using the following expression

$$m = 2\pi \int_0^R \rho(r)u(r)rdr$$

Here, R is the maximum radial distance from the centerline, where the pitot-pressure approached the atmospheric pressure value. The entrainment mass flow rate is normalized by the mass flow rate from the orifice at the exit plane. Though the entrainment mass flow rates are different for the two configurations, their variation along the longitudinal distance becomes nearly linear and attains a common slope of about 0.38 which compares well with the one reported by Mi et al [10] in their study of jet from sharp edged orifice.

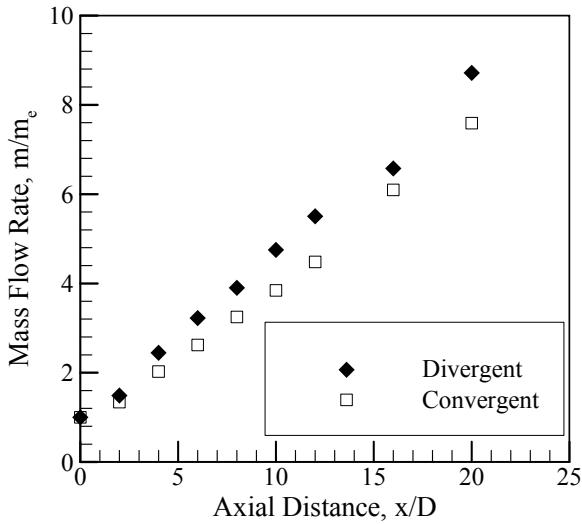


Fig. 5 Entrainment mass in the jet

The mixing layer, springing from the nozzle lip or orifice edge, has been known to govern the coherent structures responsible for the further development of jet. Therefore, to seek an explanation for the observed differences in the two jets, we decided to examine the mixing layer following the methodology proposed by Brown and Roshko [11]. Vorticity thickness, which is indicative of the mixing layer growth, was obtained at two axial locations from the velocity profiles using its maximum velocity gradient, $(\partial u/\partial r)_{\max}$, as shown in the following.

$$\delta = U_j / (\partial u/\partial r)_{\max}$$

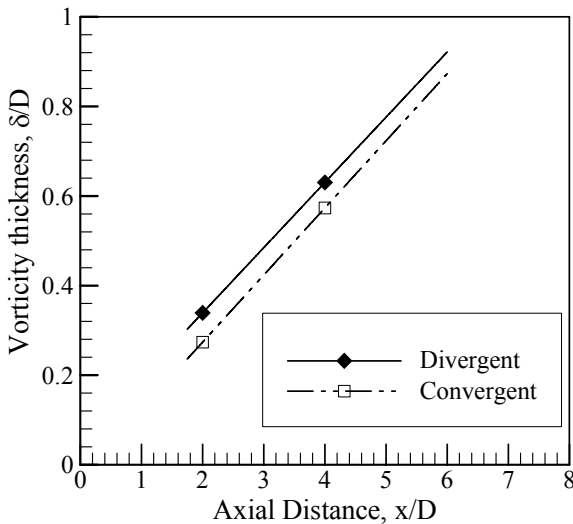


Fig. 6 Variation of vorticity thickness in mixing layer

The mixing layer thickness thus determined is plotted against the axial distance in Figure 6. It is well established from a large body of data in literature that a mixing layer, irrespective of whether it is plane or annular, grows linearly at a rate dictated by the Mach number. Therefore, it is believed that measurements of the vorticity thickness at two axial

locations will serve the purpose of comparison. Again, like the jets, the vorticity thickness in the mixing layer from the divergent orifice is distinctly more pronounced. Also, the growth rate $(\partial\delta/\partial x)$ of both the mixing layers, respectively from the convergent and the divergent orifices appears to be the same – a trend that bears similarity with the entrainment mass flow rate for the jet flows, shown in Fig. 5.

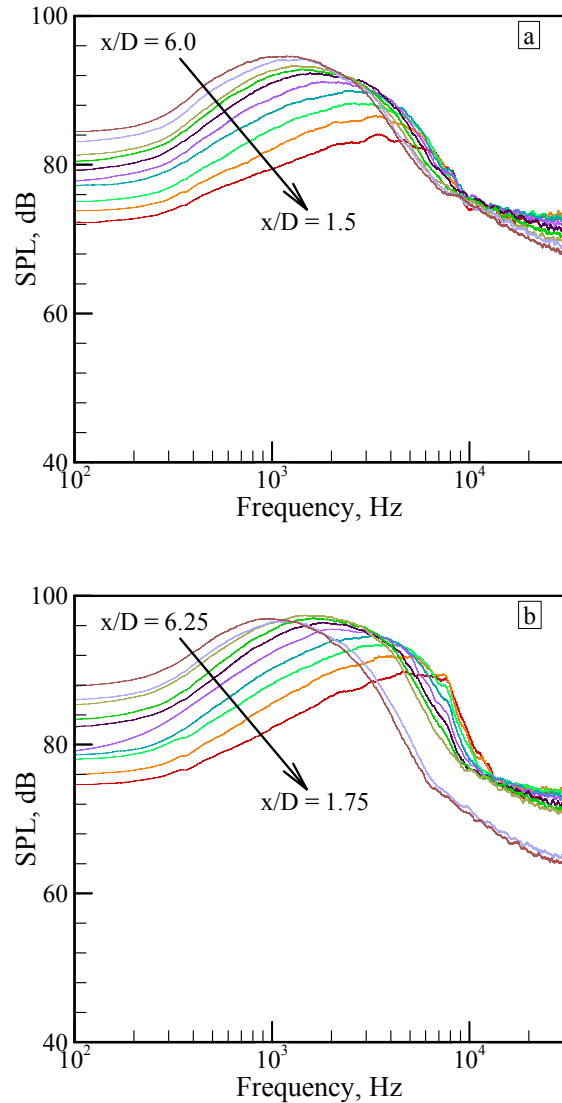


Fig. 7 Frequency spectra of acoustic pressure fluctuation along the mixing layer at $r/D=1.22$ in a step of $x/D=0.5$ (a) Divergent orifice and (b) Convergent orifice.

Figure 7 shows frequency spectra of acoustic pressure fluctuations at 10 streamwise stations, located at an interval of $0.5D$ in the first row along the mixing layer, starting from $(x/D=1.5, r/D=1.22)$ and covering the entire length of potential core. It is seen that as the distance from the orifice plate increases, the spectral peak amplitude increases and its frequency decreases. In order to appreciate the differences

between the acoustic characteristics of the two configurations tried in the present case, their spectra were plotted together on a common graph, one for each location. In Fig. 8, three such graphs are shown at selected locations. The sound pressure levels, SPL, are consistently higher over the entire frequency range for the convergent orifice, till the end of the potential core is reached at $x/D=4$. However, downstream of the potential core in the initial region of the developing jet, $x/D=6$, a cross-over of the spectra is seen at $f=3$ kHz – in the region below this frequency, the SPLs are higher for the convergent orifice and in the region above this frequency, they are higher for the divergent orifice.

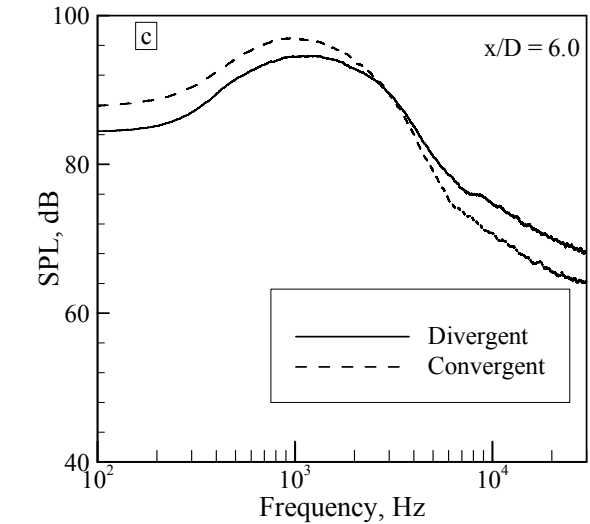
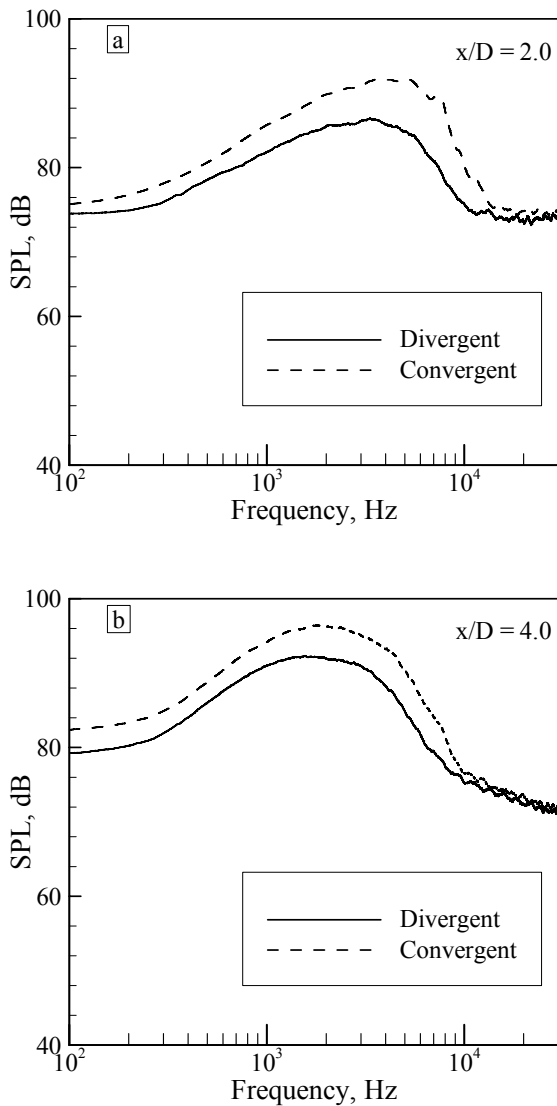


Fig. 8. Comparison of frequency spectra of acoustic pressure fluctuations taken from Fig. 7.

Figure 9 shows plots of (a) spectral peak frequency, (b) spectral peak SPL, and (c) over all sound pressure level (OASPL) along the streamwise distance from the orifice plate. Figs.9 (a) and (b) are derived from Fig. 7. It is seen that the spectral peak frequency is consistently higher for the convergent orifice till the potential core end is reached. This is consistent with the thinner mixing layer as shown in Fig. 6 – for the same convective velocity, smaller structure will produce higher frequency. It is also observed that the peak frequency continuously reduces with longitudinal distance and that is expected for a linearly growing mixing layer. Lee and Ribner [12] have reported such decay of peak frequency, within the potential core region, to be directly proportional to $1/x$. Further, thinner mixing layer, produced from the convergent orifice, contains structures with higher vorticity (stronger coherent structures) that would cause strong disturbance in the flow and hence higher noise levels. This view point is graphically supported by Fig. 9 (b) showing a monotonic difference of about 4 dB, even beyond the potential core. Fig. 9 (c) shows that the OASPL values are higher by about 40 dB compared to the peak SPL for both the orifices. Thus, the difference between their levels remains the same 4 dB.

From the acoustic data collected at all the points as shown in Fig. 3, iso-SPL contours were obtained for selected frequencies to prepare the SPL maps in the x - r plane for both the orifices. These maps are shown in Figure 10. Some interesting observations are made. The noise levels are relatively higher at lower frequencies of 1 kHz and 2 kHz, and their concentration suggests that the source of this noise is located in the region downstream of the potential core. As the frequency is increased to 5 kHz and 10 kHz, the noise levels show overall attenuation but the local maximum is seen to shift towards the orifice. Again, of the two, the SPLs for the divergent orifice are relatively lower.

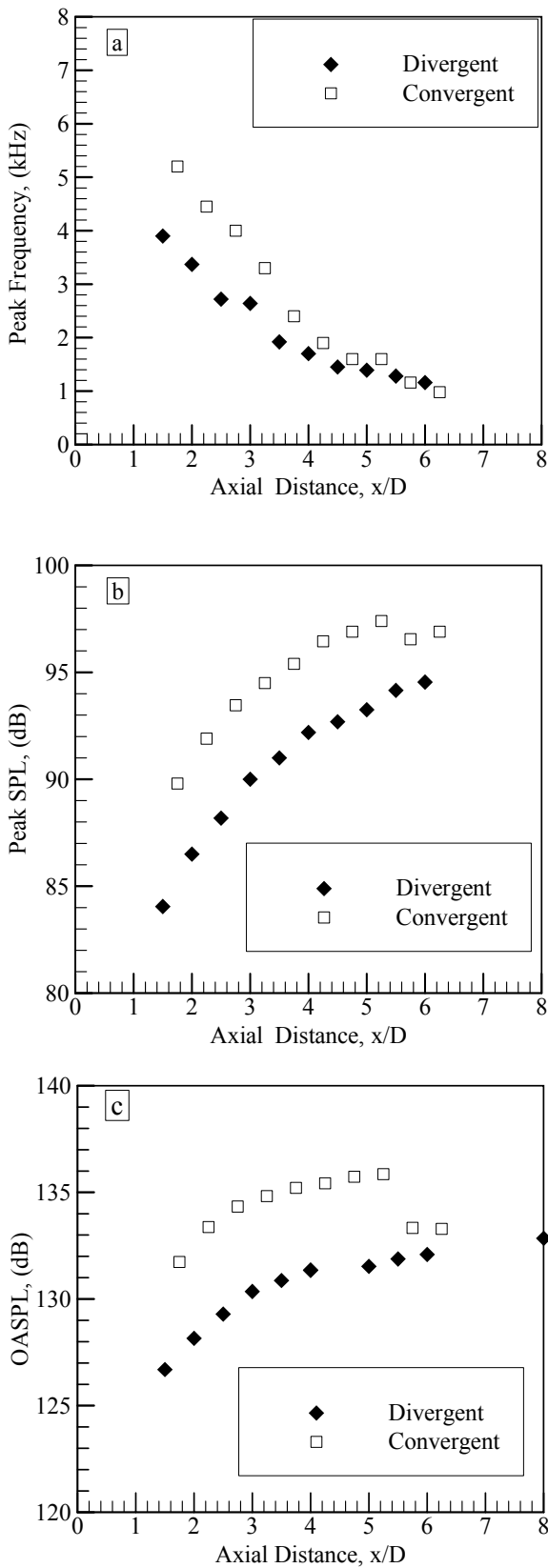


Fig. 9 Variation of (a) Spectral peak Frequency, (b) Spectral peak SPL, and (c) OASPL along the axial distance

Arndt et al.[7] proposed a technique of decomposing the near field pressure fluctuations into reactive and propagating components. They normalized the measured pressure fluctuations $(p_{rms} / \rho U_j^2)(\Delta k.D)^{-1}$ and plotted against the normalized acoustic wave number $(k.y)$, and demonstrated that the region $(k.y) < 1$ belongs to the reactive pressure field, whereas the region $(k.y) > 1$ belongs to the propagating pressure field. In the reactive pressure field, the pressure at any chosen constant frequency falls with $(k.y)^{-6}$ and in the propagating pressure field, it falls with $(k.y)^{-2}$. Following this model, the data is reduced and plotted in Fig. 11. From the close and careful observations, it is inferred that in the present case, $(k.y) \approx 3$ is the value that decides the near field and the far field. In other words, when $(k.y) < 3$, the microphone senses the near-field pressure fluctuations and when $(k.y) > 3$, the microphone senses the far-field pressure fluctuations. These plots can also be used to locate the noise source in the flow. If the microphone is just above the noise source, all the lines passing through the points of constant Strouhal numbers (normalized frequency) will have a slope of -6 in the near-field and -2 in the far field. Deviation from these slopes will mean that the microphone is placed oblique to the noise source. This is what precisely seems to be happening in the present case. Following these guidelines, it is understood that in both the cases of divergent and convergent orifices, the noise source is likely to be located in the region downstream of the potential core at about $x = 6D$.

IV. CONCLUSION

The divergent orifice is found to render faster spread of the jet with higher entrainment mass compared to the convergent orifice. Effect of the orifice geometry is seen on early development of the mixing layer – the divergent orifice resulting in thicker mixing layer. The near field acoustic measurements showed that a thin mixing layer with higher vorticity produces more noise whose peak frequency exhibited direct correlation with the scale of the structure. For the present experiments, $(k.y) \approx 3$ was found as a deciding criterion for the near field and far field pressure fluctuations. The pressure fluctuations in the region $(k.y) > 3$ are of propagating type. From the normalized pressure fluctuations and the normalized wave number plots, the noise source location was found to be in the region downstream of the potential core around 6 orifice diameters. The present results make a good case for a study to be undertaken to systematically investigate the influence of vena contracta on aerodynamic and aero-acoustic characteristics of jets.

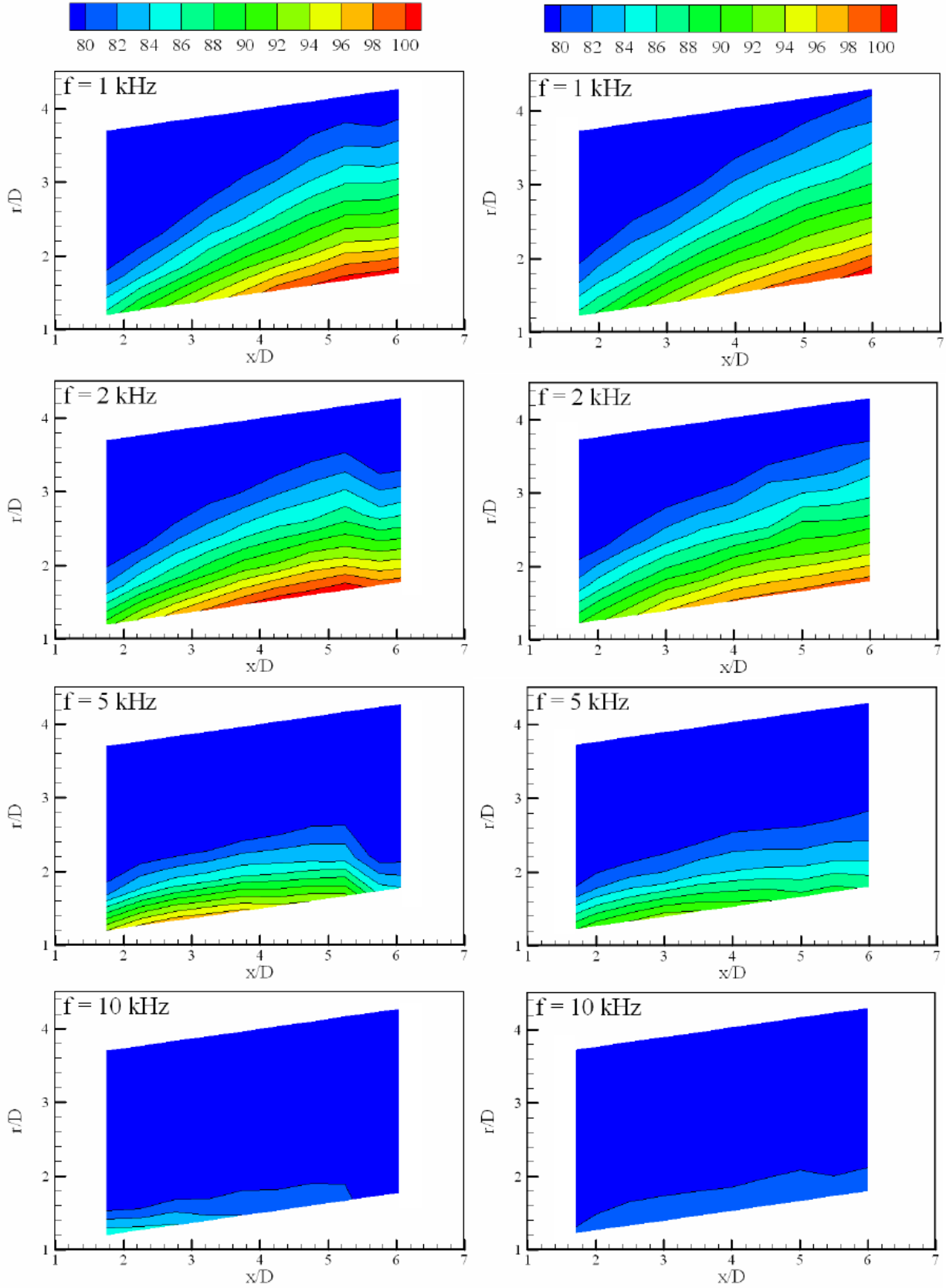


Fig. 10. Iso-SPL contours for (a) convergent and (b) divergent orifice.

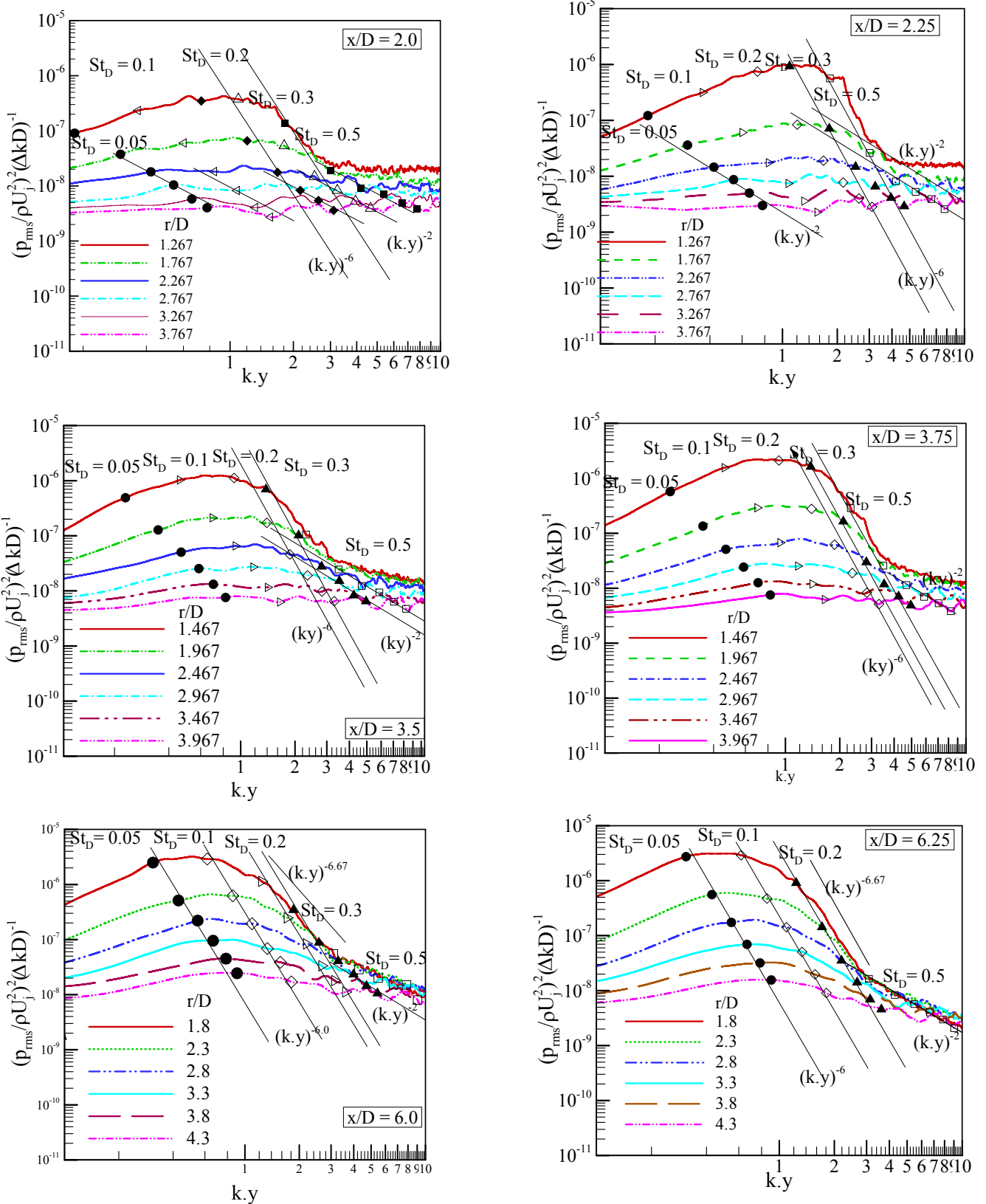


Fig. 11(a). Near field pressure fluctuations evolved from divergent orifice jet.

Fig. 11(a). Near field pressure fluctuations evolved from convergent orifice jet.

REFERENCES

- [1] K Viswanathan and L T Clark. "Effect of Internal Contour on jet aeroacoustics," in *Jet Aeroacoustics*, G. Raman, Ed. Essex UK Multi-science Pub 2008, pp. 463-495.
- [2] V. H. Arakeri, A.Krothapalli, V. Siddavaram, M B Alkislar and L M . Lourenco. "On the use of microjets to suppress turbulence in a Mach 0.9 axisymmetric jet," *Journal of Fluid Mechanics*, Vol 490, 2003, pp. 75-98.
- [3] K.B. M.Q. Zaman, "Effect of initial condition on subsonic jet noise," *AIAA Journal*, Vol 23, No. 3, 1985 pp 1370-1373.
- [4] L Maesterllo and E McDaid , Acoustic characteristic of high subsonic jet," *AIAA Journal* , Vol 9, No.6, 1971 pp 1058-1066.
- [5] K Vishwanathan, "Noise source mechanism in subsonic jets," *AIAA Journal* , Vol 46, No.8, 2008 pp 2020-2031
- [6] W R Quinn and J. Militzer "Effects of nonparallel exit flow on round turbulent free jets," *Int. J. Heat Fluid Flow* 10 (2) (1989) 139-145.
- [7] R. E. A. Arndt, D. F. Long, and M. N. Glauser, "The proper orthogonal decomposition of pressure fluctuations surrounding a turbulent jet," *Journal of Fluid Mechanics*. Vol. 340, (1997), pp. 1-33.
- [8] J. Mi, G.J. Nathan, and D Nobes, " Mixing characteristics of axisymmetric free jets issuing from contoured nozzle, an orifice plate and pipe," *Journal of Fluids Engineering* Vol 123, 2001b, pp 878-883.
- [9] W R Quinn, " Upstream nozzle shaping effects on near field flow in round turbulent free jets" *European Journal of Mechanics B/Fluids* Vol. 25, 2006 pp 279-301.
- [10] J. Mi, P. Kalt, G.J. Nathan, and C. Y. Wong, " PIV measurement of a turbulent jet issuing from round sharp-edged plate," *Experiments in Fluids*, Vol 42, 2007 pp 625-637.
- [11] G. L. Brown and A. Roshko, "On density effects and large structure in turbulent mixing layers," *Journal of Fluid Mechanics* , Vol. 64, 1974, pp 775-816.
- [12] H. K Lee and H. S Ribner, " Direct Correlation of Noise and flow field.," *Journal of Acoustic Society of America*, Vol. 52, No 5(1) 1972 pp 1280-1290.